JOURNAL OF MATERIALS SCIENCE 31 (1996) 204–208

Formation and sintering of 75 mol% alumina/25 mol% zirconia (2–3.5 mol% yttria) composite powder prepared by the hydrazine method

K. GOTO, K. HIROTA, O. YAMAGUCHI*
Department of Molecular Science and Technology, Faculty of Engineering, Doshisha University, Tanabe Kyoto 610-03, Japan
H. KUME, S. INAMURA, H. MIYAMOTO
Osaka Prefectural Institute of Industrial Technology, Osaka 550, Japan

Al_2O_3/Y_2O_3-doped ZrO_2 composite powders with 25 mol% ZrO_2 have been prepared by the hydrazine method. As-prepared powders are the mixtures of AlO(OH) gel solid solutions and amorphous ZrO_2. The formation process leading to α-Al_2O_3/t-ZrO_2 composite powders is investigated. Hot isostatic pressing has been performed for 1 h at 1500 °C under 196 MPa. Dense ZrO_2-toughened Al_2O_3 (ZTA) ceramics with homogeneous-dispersed ZrO_2 particles show excellent mechanical properties. The toughening mechanism is discussed.

1. Introduction

Zirconia-toughened alumina (ZTA), in which ZrO_2 is present as a secondary dispersed phase, has attracted much scientific and technological interest in recent years because of its enhanced toughness and strength. The mechanical properties of ZTA depend mainly on the amount of ZrO_2 addition, the size of ZrO_2 grains, and the relative content of t-ZrO_2. Two important mechanisms, i.e. microcrack toughening [1, 2] and stress-induced transformation toughening [3, 4] have been proposed to explain the increased toughness of ZTA. The former and the latter are the major phenomenon when the dispersed ZrO_2 particles are monoclinic and tetragonal, respectively. To improve the mechanical properties of ZTA, various approaches, such as mechanical mixing of powders [5], reactive sintering [5], hot isostatic pressing [6], sol–gel synthesis [7], evaporative decomposition of slurry [8], and spray-ion-coupled plasma (ICP) technique [9], have been reported in the literature. It has previously been reported that in the ZrO_2–Al_2O_3 system, a new powder preparation method using hydrazine monohydrate was developed for the formation and sintering of composite powders up to 50 mol% Al_2O_3 [10, 11]. In a further recent study [12], we reported that AlO(OH) gel solid solutions containing up to $\approx$10 mol% ZrO_2 were formed. The present paper deals with the formation and sintering of 75 mol% Al_2O_3–25 mol% ZrO_2 (2–3.5 mol% Y_2O_3) composite powders prepared by the hydrazine method.

2. Formation

Four compositions, denoted A–D, were chosen for this study (Table I). Anhydrous aluminium chloride ($AlCl_3$, 99.9% pure), anhydrous zirconium chloride ($ZrCl_4$, 99.9% pure), yttrium chloride ($YCl_3 \cdot 6H_2O$, 99.95% pure), and hydrazine monohydrate ($(NH_2)_2 \cdot H_2O$, 80%) were used as starting materials. The first two and the third were adjusted in concentrations of 0.5 mol l^{-1} and 0.1 mol l^{-1} aqueous solutions, respectively, by dissolving in distilled water. The mixed aqueous solution (pH = 2) was stirred with a magnetic stirrer for 30 min at room temperature, and then hydrazine monohydrate was added dropwise to the mixed solution at 60 °C, with stirring, until the resulting suspension reached pH = 8. After completion of the addition, the suspension was heated for 1 h at the same temperature. The products were separated from the suspensions by centrifugation, washed more than ten times in hot water to remove adsorbed hydrazine and chloride ions (tested by adding a silver nitrate solution), and then dried at 120 °C under reduced pressure. The average particle size of the starting powders, determined by transmission electron microscopy (TEM), was $\approx$5 nm (Fig. 1).

The starting powders and heated specimens were examined by X-ray diffraction (XRD) using nickel-filtered CuK_α radiation. All starting powders showed the XRD patterns of AlO(OH) gel as shown in Fig. 2a, although the lines were weak in intensity in comparison with those of pure AlO(OH) gel (Fig. 2b) prepared by the present method. Differential thermal analysis

* Author to whom all correspondence should be addressed.

0022–2461

TABLE I Chemical composition of starting powders

Starting powder	Composition (mol %)	
	$Al_2O_3/ZrO_2/Y_2O_3$	$Y_2O_3/(ZrO_2 + Y_2O_3)$
A	75/24.50/0.50	2.0
B	75/24.38/0.62	2.5
C	75/24.25/0.75	3.0
D	75/24.13/0.87	3.5

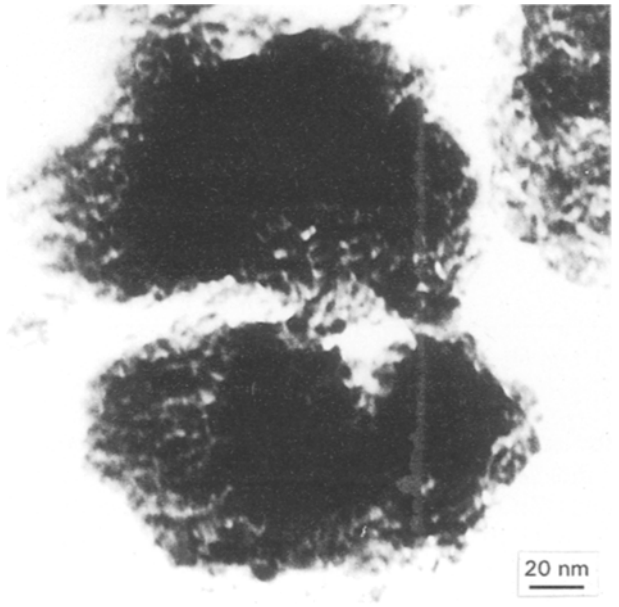

Figure 1 Transmission electron micrograph of powder C.

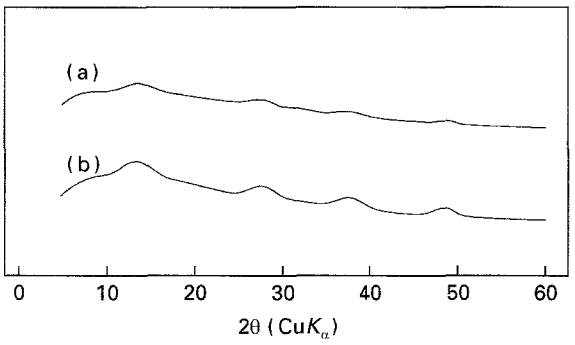

Figure 2 X-ray diffraction patterns for (a) powder C, and (b) pure AlO(OH) gel.

(DTA) was conducted in air at a heating rate of 10 °C min^{-1}; α-Al_2O_3 was used as the reference. The DTA curve of powder C is shown in Fig. 3. Other starting powders gave the same curve as with powder C. Two successive endothermic peaks below 400 °C can be attributed to the dehydration of absorbed water and hydrated water. An endothermic peak at 400–550 °C resulted from the release of the hydroxyl group from AlO(OH) gel. Exothermic peaks at 860–960 °C and 1275–1375 °C, as will be described, were found to result from the crystallization of t-ZrO_2 and the transformation of θ- to α-Al_2O_3, respectively.

Table II shows the phase developments with increasing temperature for powder C. During the course

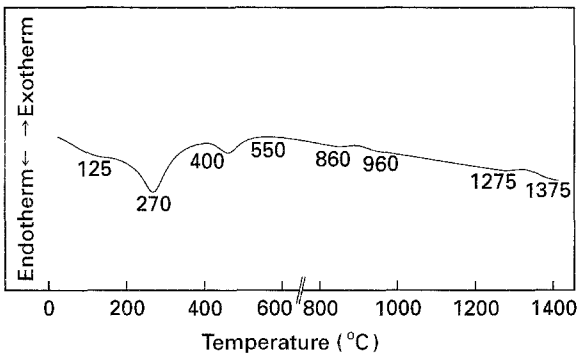

Figure 3 DAT curve for powder C.

of dehydration of AlO(OH) gel, it became amorphous to X-rays. No significant changes in structure were observed up to 750 °C. γ-Al_2O_3 and t-ZrO_2 crystallized slowly above 750 °C and at 860–960 °C, respectively. The latter phase grew rapidly above 1100 °C with the transformation of γ- to θ-Al_2O_3. A sample, of composition of 90 Al_2O_3/10 ZrO_2 (3 Y_2O_3) mol %, was prepared by the present method. This sample is termed "sample z". No peak resulting from the crystallization of t-ZrO_2 in this sample was observed in the DTA curve. This result suggests that sample z was AlO(OH) gel solid solution containing ZrO_2. Accordingly, it can be concluded that the starting powders were the mixtures of AlO(OH) gel solid solution and amorphous ZrO_2. Fig. 4 shows the intensity of the main characteristic XRD line (1 1 1) of t-ZrO_2 with increasing temperature for powder C and sample z. The important fact in powder C is that the formation of t-ZrO_2 proceeded in two steps: (I) crystallization of free amorphous ZrO_2 and (II) decomposition of γ-Al_2O_3 solid solution. The γ- to θ-Al_2O_3 transformation occurred slowly at 1100–1310 °C. The formation of α-Al_2O_3 was recognized above 1275 °C. A composite powder of α-Al_2O_3 and t-ZrO_2 was produced when heated at 1375 °C. The lattice parameter of γ-Al_2O_3 from each starting powder, as well as in AlO(OH) gel, could not be determined, because of its weak and wide XRD lines. From the results of DTA and XRD analysis, the reaction process can be summarized as shown in Fig. 5.

3. Sintering

Sintering was performed by hot isostatic pressing (HIP) using argon gas as the pressure-transmitting medium. Before HIP, the α-Al_2O_3/t-ZrO_2 composite powders were prepared by calcining for 1 h at 1350 °C. They were pressed into pellets at 196 MPa and then isostatically cold-pressed at 392 MPa. The green compacts, covered with boron nitride powder, were sealed in a Pyrex-glass tube under vacuum. HIPing conditions were as follows: (1) heating rate of 400 °C h^{-1}, (2) increasing pressure rate of $\approx$180 MPa h^{-1} above 800 °C, and (3) sintering for 1 h at 1500 °C under 196 MPa. Table III shows the characteristics of the sintered ZTA. Bulk densities, after lapping with a diamond powder, were verified by the Archimedes' method. They showed a constant value ($\approx$4.41 g cm^{-3})

TABLE II Phases identified for specimens quenched after heating to various temperatures for powder C

Phase identified						
550–750 °C	750–860 °C	860–1100 °C	1100–1275 °C	1275–1310 °C	1310–1375 °C	1375–1400 °C
Amorphous	γ-Al_2O_3	γ-Al_2O_3 t-ZrO_2	γ-Al_2O_3 θ-Al_2O_3 t-ZrO_2	γ-Al_2O_3 θ-Al_2O_3 α-Al_2O_3 t-ZrO_2	θ-Al_2O_3 α-Al_2O_3 t-ZrO_2	α-Al_2O_3 t-ZrO_2

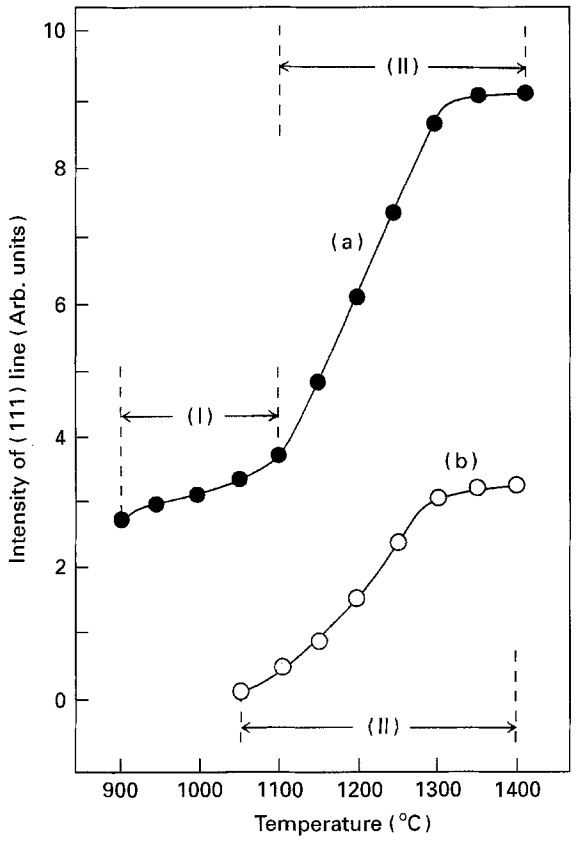

Figure 4 Intensity of the (1 1 1) line for t-ZrO_2 from (a) powder C, and (b) sample z.

regardless of the starting composition. The contents of t-ZrO_2 (m-ZrO_2) in ZTA were measured by the XRD technique on the fracture surfaces [13]. The ZTA with 2 and 2.5 mol % Y_2O_3 contained the m-ZrO_2 phase; the contents were 14 and 8 vol % for the former and

TABLE III Characteristics of ZTA ceramics

Starting powder	Bulk density ($g\,cm^{-3}$)	Phase[a]
A	4.41	α-Al_2O_3, t, m(14 vol %)
B	4.41	α-Al_2O_3, t, m(8 vol %)
C	4.41	α-Al_2O_3, t
D	4.40	α-Al_2O_3, t $\geqslant$ C

[a] t = t-ZrO_2, m = m-ZrO_2, and C = C-ZrO_2.

the latter materials, respectively. The ZTA containing 3 mol % Y_2O_3 was a composite material of α-Al_2O_3 and t-ZrO_2. The relative density of the ZTA estimated from the theoretical densities of α-Al_2O_3 and t-ZrO_2 (3 mol % Y_2O_3) [14] was 99.8%. For the 3.5 mol % Y_2O_3 composition, a very small amount of c-ZrO_2 was present in addition to the two other phases. Fig. 6 shows scanning electron micrographs for the fracture surfaces of ZTA. Microstructures were changed little for compositions; the grain size of α-Al_2O_3 was 1.5 μm and intergranular and intragranular ZrO_2 of 0.47 μm and 0.3 μm in sizes, respectively, were observed.

After the sintered ZTA materials were cut with a diamond saw, they were lapped with a diamond powder (nominal size 1–2 μm). Test-bar samples for mechanical measurements were 3 mm high, 3 mm wide, and 20 mm long. The fracture toughness, K_{IC}, measurements were made by the microindentation technique [15, 16] with a 490 N Vickers load. Three-point bending strength was measured with a 16 mm span and a crosshead speed of 0.5 mm min^{-1}. Fig. 7 shows the K_{IC} and bending strength of ZTA as a function of Y_2O_3 addition. The K_{IC} decreased linearly from 6.6 to 5.5 MPa $m^{1/2}$ with increased Y_2O_3

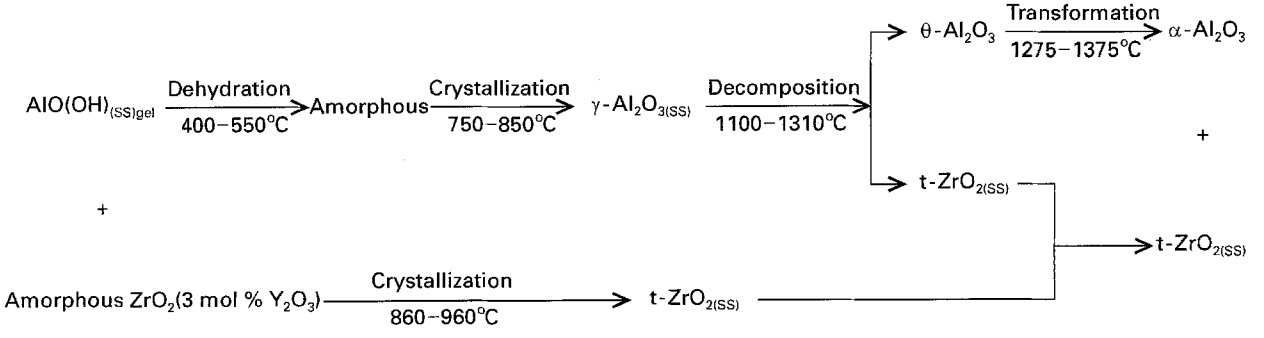

Figure 5 Reaction process leading to α-Al_2O_3–t-ZrO_2 composite powder.

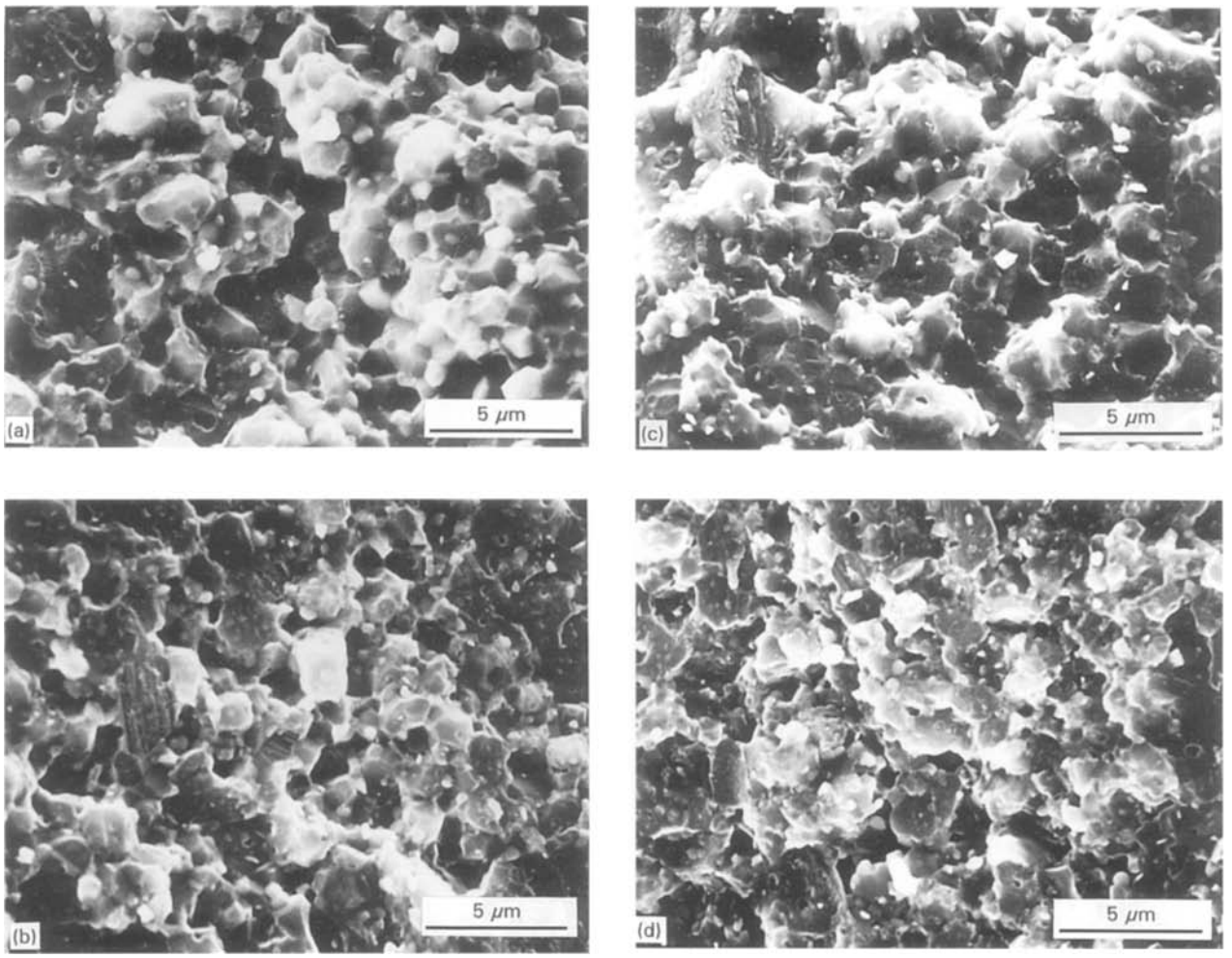

Figure 6 Scanning electron micrographs for fracture surfaces of ZTA ceramics from powders (a) A, (b) B, (c) C, and (d) D.

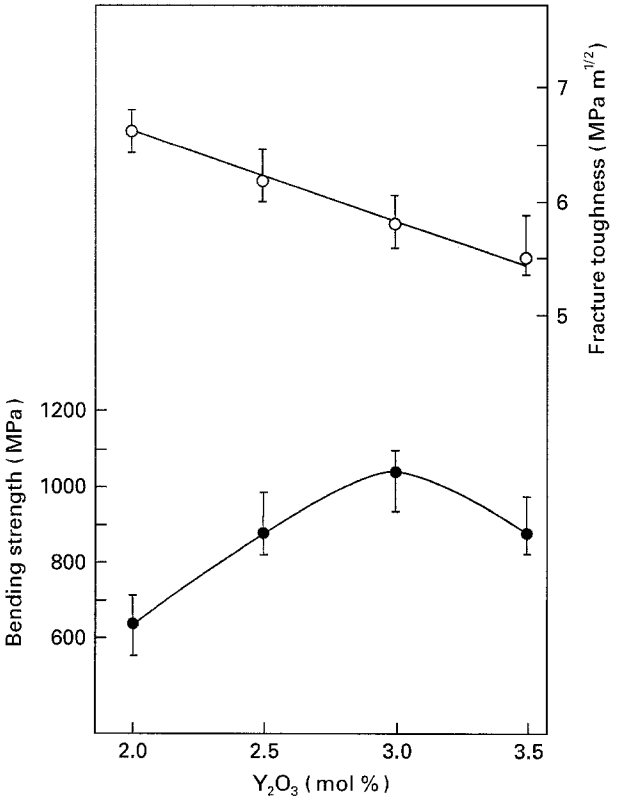

Figure 7 (○) Fracture toughness and (●) bending strength of ZTA ceramics as a function of Y_2O_3 addition.

addition. The behaviour of K_{IC} agreed with data (6.7–4.8 MPa $m^{1/2}$) reported previously [17]. As described earlier, the t- and m-ZrO_2 particles enhanced the toughness by creating the stress-induced transformation toughening [3, 4] and by extending the pre-existing microcracks [1, 2], respectively. Accordingly, the major toughening mechanism in this study was probably stress-induced transformation toughening, and the contribution of the microcrack extension was relatively small. The average strength of the ZTA with 2 mol % Y_2O_3 was 638 MPa. It increased to the maximum of 1050 MPa with 3 mol % Y_2O_3. The results can be explained in terms of the increased t-ZrO_2 phase (86 → 92 → 100 vol %) with increased Y_2O_3 addition. The strength decreased in the ZTA with 3.5 mol % Y_2O_3. This effect is probably due to the presence of c-ZrO_2 in which the strength is weak. Lange [18, 19] fabricated ZTA ceramics in the composition of up to 30 vol % (35.2 mol %) ZrO_2 with 2 mol % Y_2O_3 and in 30 vol % ZrO_2 with 3 mol % Y_2O_3 using submicrometre-sized powders prepared by ball-milling. Sintering techniques were hot-pressing (1600 °C/2 h) [18] and post-HIP (1500 °C/200 MPa/1 h) [19]. For this earlier work, the maximum strength was 869 MPa in the ZTA fabricated from the 70 vol % Al_2O_3/30 vol % ZrO_2 (3 mol % Y_2O_3) powder. Becher [17] prepared the composite powder with the

same composition as described by Lange [19] by a sol–gel technique and reported that the strength of the ZTA fabricated by vacuum hot-pressing (1425–1550 °C) was 740 MPa. Thus, the ZTA ceramics from powder C in the present study were found to show excellent mechanical strength.

4. Conclusions

Composite powders with 75 mol % Al_2O_3/25 mol % ZrO_2 (2–3.5 mol % Y_2O_3) have been prepared by the hydrazine method. As-prepared powders are the mixtures of AlO(OH) gel solid solutions and amorphous ZrO_2. Reaction process leading to α-Al_2O_3/t-ZrO_2 composite powders can be summarized as shown in Fig. 5. ZTA ceramics (99.8% of theoretical) containing 3 mol % Y_2O_3 have been fabricated by hot isostatic pressing for 1 h at 1500 °C and 196 MPa. The texture shows the microstructure consisting of homogeneous-dispersed fine ZrO_2 particles. The ZTA gives 5.8 MPa $m^{1/2}$ and 1050 MPa for fracture toughness and bending strength, respectively. The results present the excellent mechanical properties.

References

1. A. G. EVANS and K. T. FABER, *J. Am. Ceram. Soc.* **64** (1981) 394.
2. *Idem, ibid.* **67** (1984) 255.
3. R. McMEEKING and A. G. EVANS, *ibid.* **65** (1982) 242.
4. B. BUDIANSKY, J. W. HUTCHINSON and J. C. LAMBROPOULOS, *Int. J. Solids Struct.* **19** (1983) 337.
5. N. CLAUSSEN and M. RÜHLE, in "Advances in Ceramics", Vol. 3 (American Ceramic Society, Columbus, OH, 1981) p. 137.
6. S. HORI, M. YOSHIMURA and S. SŌMIYA, *J. Am. Ceram. Soc.* **69** (1986) 169.
7. A. H. HEUER, N. CLAUSSEN, W. M. KRIVEN and M. RÜHLE, *ibid.* **65** (1982) 642.
8. D. W. SPROSON and G. L. MESSING, *ibid.* **67** (1984) C-92.
9. M. KAGAWA, M. KIKUCHI, Y. SYONO and T. NAGAE, *ibid.* **66** (1983) 751.
10. K. ISHIDA, K. HIROTA, O. YAMAGUCHI, K. KUME, S. INAMURA and H. MIYAMOTO, *ibid.* **77** (1994) 1391.
11. S. KIMOTO, K. HIROTA, O. YAMAGUCHI, H. KUME, S. INAMURA and H. MIYAMOTO, *ibid.* **77** (1994) 1694.
12. K. YAMAKATA, K. HIROTA, O. YAMAGUCHI, H. KUME, S. INAMURA and H. MIYAMOTO, *ibid.* **77** (1994) 2207.
13. R. C. GARVIE and P. S. NICHOLSON, *ibid.* **55** (1972) 303.
14. S. HORI, M. YOSHIMURA, S. SŌMIYA, R. KURITA and H. KAJI, *J. Mater. Sci. Lett.* **4** (1985) 413.
15. A. G. EVANS and E. A. CHARLES, *J. Am. Ceram. Soc.* **59** (1976) 371.
16. K. NIIHARA, A. NAKAHIRA and T. HIRAI, *ibid.* **67** (1984) C-13.
17. P. F. BECHER, *Zirconia Ceram.* **1** (1983) 151.
18. F. F. LANGE, *J. Mater. Sci.* **17** (1982) 247.
19. *Idem, J. Am. Ceram. Soc.* **66** (1983) 396.

Received 15 April 1994
and accepted 22 June 1995